Initialization of the Shooting Method via the Hamilton-Jacobi-Bellman Approach

Article *in* Journal of Optimization Theory and Applications · August 2010

DOI: 10.1007/s10957-010-9649-6 · Source: arXiv

2 authors:

Emiliano Cristiani
Italian National Research Council
96 PUBLICATIONS **1,494** CITATIONS
SEE PROFILE

Pierre Martinon
National Institute for Research in Computer Science and Control
56 PUBLICATIONS **807** CITATIONS
SEE PROFILE

J Optim Theory Appl
DOI 10.1007/s10957-010-9649-6

Initialization of the Shooting Method via the Hamilton-Jacobi-Bellman Approach

E. Cristiani · P. Martinon

Abstract The aim of this paper is to investigate from the numerical point of view the coupling of the Hamilton-Jacobi-Bellman (HJB) equation and the Pontryagin minimum principle (PMP) to solve some control problems. A rough approximation of the value function computed by the HJB method is used to obtain an initial guess for the PMP method. The advantage of our approach over other initialization techniques (such as continuation or direct methods) is to provide an initial guess close to the global minimum. Numerical tests involving multiple minima, discontinuous control, singular arcs and state constraints are considered.

Keywords Optimal control problems · Minimum time problems · Hamilton-Jacobi-Bellman equations · Pontryagin minimum principle · Shooting method

1 Introduction

In optimal control, the so-called direct methods, based on discretization and nonlinear programming, are currently the most popular. The development of many powerful codes in the recent years, such as NUDOCCCS [1], MUSCOD [2], or IPOPT [3],

Communicated by H.J. Pesch.

E. Cristiani (✉)
CEMSAC, Università di Salerno, Fisciano SA, Italy
e-mail: emiliano.cristiani@gmail.com

E. Cristiani
IAC-CNR, Rome, Italy

P. Martinon
INRIA and CMAP École Polytechnique, Palaiseau, France
e-mail: martinon@cmap.polytechnique.fr

Published online: 18 February 2010

has allowed to solve difficult and complex problems [4, 5]. On the other hand, the indirect methods, based on the Pontryagin minimum principle (PMP), are both fast and accurate, but tend to suffer from great sensitivity to the initialization. The aim of this paper is to show that this difficulty can be overcome by coupling the indirect methods with the Hamilton-Jacobi-Bellman (HJB) approach.

HJB theory and PMP are usually considered two separate worlds, although they deal with the same kind of problems. The theoretical connections between the two approaches are well known [6–9]; coupled usage of the two techniques is not common and is not completely explored. In this paper, we deal with the following controlled dynamics:

$$\begin{aligned} &\dot{y}(t) = f(y(t), u(t)), \quad t > 0, \\ &y(0) = x, \quad x \in \mathbb{R}^d, \end{aligned} \tag{1}$$

where the control variable $u \in \mathcal{U} := \{u : \mathbb{R}^+ \to U,\ u \text{ measurable}\}$ and $U \subset \mathbb{R}^m$ ($m \geq 1$). We denote by $y_x(t; u)$ the solution of the system (1) starting from the point x with control u. Let $\mathcal{C} \subset \mathbb{R}^d$ be a given *target*. For any given control u, we denote by $t_f(x, u)$ the first time the trajectory $y_x(t; u)$ hits $\mathcal{C}$ (we set $t_f(x, u) = +\infty$, if the trajectory never hits the target). We also define a *cost functional* J as

$$J(x, u) := \int_0^{t_f(x,u)} \ell(y_x(t; u), u(t))dt, \tag{2}$$

where ℓ is a suitable cost function. The final goal is to find

$$u^* \in \mathcal{U} \quad \text{such that} \quad J(x, u^*) = \min_{u \in \mathcal{U}} J(x, u), \tag{3}$$

and compute the associated optimal trajectory $y_x^*(t; u^*)$.

Finally, we define the *value function*

$$\mathcal{T}(x) := J(x, u^*), \quad x \in \mathbb{R}^d.$$

Choosing $\ell \equiv 1$ in (2), we obtain the classical *minimum time* problem.

The PMP approach consists in finding a trajectory which satisfies some necessary conditions. This is done in practice by searching for the zero of a certain shooting function, typically with a quasi-Newton method. This method is well known and it is used in many applications [10–12 and references therein]. The main advantages of this approach lie in accuracy and low numerical complexity. It is worth to recall that the dimension of the nonlinear system for the shooting method is usually $2d$, where d is the state dimension. In practice, this is quite low for this kind of problem; therefore, fast convergence is expected in case of success, especially if the initial guess is close to the right value. Unfortunately, finding a suitable initial guess can be extremely difficult in practice. The algorithm might not converge at all or might converge to a local minimum of the cost functional.

The HJB approach is based on the dynamic programming principle [13]. It consists in characterizing the value function $\mathcal{T}$ as the solution of a first-order nonlinear

partial differential equation. Once an approximation of the value function is computed, one can easily obtain both the optimal control u^* in feedback form and, by direct integration, the optimal trajectories for any starting point $x \in \mathbb{R}^d$ [14, 15]. The method is greatly advantageous because it is able to reach the global minimum of the cost functional, even if the problem is not convex. The HJB approach allows also to have a global overview of the optimal trajectories and the reachable sets (or capture basins), i.e. the sets of points from which it is possible to reach the target in any given time. Beside all the advantages listed above, the HJB approach suffers from the well known "curse of dimensionality", so in general it is restricted to problems in low dimension ($d \leq 3$).

In this paper, we couple the two methods in such a way that we can preserve the respective advantages. The idea is to solve the problem via the HJB method on a coarse grid, to have in short time a first approximation of the value function and the structure of the optimal trajectory. Then, we use this information to initialize the PMP method and compute a precise approximation of the global minimum. To our knowledge, this is the first attempt to exploit the connection between the HJB and PMP theories from the numerical point of view.

Compared to the use of continuation techniques or direct methods to obtain an estimate of the initial costate, the main advantage of the approach presented here is that the HJB method provides an initial guess close to the global minimum. The main limitation is the restriction with respect to the dimension of the state.

We consider some known control problems with different specific difficulties: several local minima, several global minima, discontinuous control, presence of singular arcs, and state constraints. In all these problems, we show that combining the PMP method with the HJB approach leads to a very efficient algorithm.

2 Preliminaries

We consider optimal control problems in general Bolza form, autonomous case, with either a fixed or free final time,

$$
\begin{aligned}
(\mathrm{P}) \quad \min \quad & J(x,u) = \int_0^{t_f(x,u)} \ell(y(t),u(t))dt \quad \text{(Objective)} \\
\text{s.t.} \quad & \dot{y}(t) = f(y(t),u(t)) \quad \text{(Dynamics)} \\
& u(t) \in U, \quad t \in (0, t_f(x,u)) \quad \text{(Admissible Control)} \\
& y(0) = x \quad \text{(Initial Condition)} \\
& y(t_f(x,u)) \in \mathcal{C} \quad \text{(Final Condition).}
\end{aligned}
$$

Here, U is a compact set of $\mathbb{R}^m$ and the following classical assumptions are made:

(i) $f : \mathbb{R}^d \times U \to \mathbb{R}^d$ and $\ell : \mathbb{R}^d \times U \to \mathbb{R}$ are continuous and are of class C^1 with respect to the first variable.

(ii) $\mathcal{C}$ is a closed subset of $\mathbb{R}^d$ for which the property "a vector is normal to $\mathcal{C}$ at a point of $\mathcal{C}$" makes sense. For instance, $\mathcal{C}$ can be described by a finite set of equalities $\{c_i(x) = 0\}_i$ or inequalities $\{c_i(x) \leq 0\}_i$, with c_i being of class C^1 for

every i. The classical constraint qualification assumptions hold. For numerical purposes, we assume that $\mathcal{C}$ is bounded.

2.1 Pontryagin Minimum Principle Approach

We give here a brief overview of the so-called indirect methods for optimal control problems [16–18]. We introduce the costate p, of same dimension d as the state x, and define the Hamiltonian

$$H(y, p, u, p_0) = p_0 \ell(y, u) + \langle p, f(y, u) \rangle.$$

Under the assumptions on f and ℓ introduced above, the Pontryagin minimum principle states that, if (y_x^*, u^*, t_f^*) is a solution of (P), then there exists $(p_0, p^*) \neq 0$ absolutely continuous such that

$$\begin{aligned}
&\dot{y}^*(t) = H_p(y_x^*(t), p^*(t), u^*(t), p_0), \qquad y_x^*(0) = x,\\
&\dot{p}^*(t) = -H_y(y_x^*(t), p^*(t), u^*(t), p_0),\\
&p^*(t_f^*) \perp T_{\mathcal{C}}(y_x^*(t_f^*)),\\
&u^*(t) = \arg\min_{v \in U} H(y_x^*(t), p^*(t), v, p_0), \quad t \in [0, t_f^*],
\end{aligned}$$

where $T_{\mathcal{C}}(\xi)$ denotes the contingent cone of $\mathcal{C}$ at ξ. Moreover, if the final time t_f^* is not fixed and is an optimal time, then we have the additional condition:

$$H(y_x^*(t), p^*(t), u^*(t), p_0) = 0, \quad \text{for } t \in (0, t_f^*). \tag{4}$$

Two common cases are $\mathcal{C} = \{y_f\}$ with $p^*(t_f^*)$ free and $\mathcal{C} = \mathbb{R}^d$ with $p^*(t_f^*) = 0$.

Now we assume that minimizing the Hamiltonian provides the control as a function γ of the state and costate. For a given value of $p(0)$, we can integrate (y, p) by using the control $u = \gamma(y, p)$ on $[0, t_f]$. We define the shooting function S that maps the unknown $p(0)$ to the value of the final and transversality conditions at $(y(t_f), p(t_f))$. Finding the zero of S gives a trajectory (y, u) that satisfies the necessary conditions for the problem (P). This is typically done in practice by applying a quasi-Newton method.

Remark 2.1 The multiplier p_0 could be equal to 0. In that case, the PMP is said abnormal, its solution (y^*, p^*, u^*) corresponds to a singular extremal, which does not depend on the cost function ℓ. Several works have been devoted to the existence or nonexistence of such extremal curves [19, 20]. For numerics, in general we assume that $p_0 \neq 0$, which leads to solving the PMP system with $p_0 = 1$. In the sequel, we always assume that we are in the normal case ($p_0 = 1$).

Singular Arcs A singular arc occurs when minimizing the Hamiltonian fails to determine the optimal control u^* on a whole time interval. The typical context is when H is linear with respect to u, with an admissible set of controls of the form $U =$

$[u_{\text{low}}, u_{\text{up}}]$. In this particular case, the function $(y, p, u) \longmapsto H_u(y, p, u)$ does not depend on the control variable. We define the switching function $\psi(y, p) = H_u(y, p, u)$ and have the following bang-bang control law:

$$\begin{aligned} &\text{if } \psi(y, p) > 0, \quad \text{then } u^* = u_{\text{low}}, \\ &\text{if } \psi(y, p) < 0, \quad \text{then } u^* = u_{\text{up}}, \\ &\text{if } \psi(y, p) = 0, \quad \text{then switching or singular control.} \end{aligned}$$

A singular arc then corresponds to a time interval where the switching function ψ is zero. The usual way to obtain the singular control is to differentiate ψ with respect to t until the control appears explicitly, which leads to solving an equation of the form $\psi^{(2k)}(y, p) = 0$; see [17]. This step can be quite difficult in practice, depending on the problem. Moreover, it is also required to make assumptions about the control structure, more precisely to fix the number of singular arcs. Each expected singular arc adds two shooting unknowns $(t_{\text{entry}}, t_{\text{exit}})$, with the corresponding junction conditions $\psi(t_{\text{entry}}) = \dot{\psi}(t_{\text{entry}}) = 0$ or alternatively $\psi(t_{\text{entry}}) = \psi(t_{\text{exit}}) = 0$. The problem studied in Sect. 7 presents such a singular arc.

State Constraints We consider a state variable inequality constraint $g(y(t)) \leq 0$. We denote by q the smallest order such that $g^{(q)}$ depends explicitly on the control u; q is called the order of the constraint function g. The Hamiltonian is defined with an additional term for the constraint,

$$H(y, p, u) = \ell(y, u) + \langle p, f(y, u) \rangle + \mu g^{(q)}(y, u),$$

with the sign condition

$$\begin{aligned} &\mu = 0, \quad \text{if } g < 0, \\ &\mu \geq 0, \quad \text{if } g = 0. \end{aligned}$$

When the constraint is inactive we are in the same situation as for an unconstrained problem. Over a constrained arc where $g(y) = 0$, we obtain the control from the equation $g^{(q)}(y, u) = 0$ and μ from the equation $H_u = 0$. As in the singular arc case, we need to make assumptions concerning the control structure, namely the number of constrained arcs. Each expected constrained arc adds two shooting unknowns $(t_{\text{entry}}, t_{\text{exit}})$ with the Hamiltonian continuity as corresponding conditions. We also have the so-called tangency condition at the entry point,

$$N(y(t_{\text{entry}})) := (g(y(t_{\text{entry}})), \ldots, g^{(q-1)}(y(t_{\text{entry}}))) = 0,$$

with the costate discontinuity

$$p(t_{\text{entry}}^+) = p(t_{\text{entry}}^-) - \pi N_y(y(t_{\text{entry}})),$$

where $\pi \in \mathbb{R}^q$ is another multiplier yielding an additional shooting unknown.

Remark 2.2 The tangency condition can also be enforced at the exit time. In this case, the costate jump occurs at the exit time as well.

2.2 Hamilton-Jacobi-Bellman Approach

Consider the value function $\mathcal{T} : \mathbb{R}^d \to \mathbb{R}$, which maps every initial condition $x \in \mathbb{R}^d$ to the minimal value of problem (P). It is well known (see for example [21] for a comprehensive introduction) that the value function $\mathcal{T}$ satisfies a dynamic programming principle and that the Kružkov transform of $\mathcal{T}$, defined by

$$v(x) := 1 - e^{-\mathcal{T}(x)},$$

is the unique solution in *viscosity* sense [21] of the following HJB equation:

$$\begin{aligned} &v(x) + \sup_{u \in U}\{-f(x,u) \cdot Dv(x) - \ell(x,u) + (\ell(x,u) - 1)v(x))\} = 0, \quad x \in \mathbb{R}^d \backslash \mathcal{C}, \\ &v(x) = 0, \quad x \in \mathcal{C}. \end{aligned} \tag{5}$$

Obtaining a numerical approximation of the function v is a difficult task, mainly because v is not always differentiable. Several numerical schemes have been studied in the literature. In this paper, we use a first-order semi-Lagrangian (SL) scheme [14, 15]. This choice is motivated by the fact that the SL scheme seems the best one in order to approximate the gradient of the value function, this being our goal as we will see in the next section. More precisely, a first-order finite-difference scheme is less accurate (but faster) because is not able to follow the characteristics along diagonal directions, its stencil being limited to the four neighbouring nodes (plus the considered node itself); see for example [22]. The Ultra-Bee scheme is accurate, but the solution is quite stair-shaped and not suitable for the approximation of the partial derivatives; see for example [23, 24].

We fix a (numerical) bounded domain $\Omega \supset \mathcal{C}$ and we discretize it by means of a regular grid $G = \{x_i, i = 1, \ldots, N_G\}$, where N_G is the total number of nodes. We denote by $\widetilde{v}(x; h, k, \Omega)$ the fully discrete approximation of v, with h and k being two discretization parameters (the first one can be interpreted as a time step to integrate along characteristics and the second one is the usual space step). We impose state constraint boundary conditions on $\partial\Omega$. The discrete version of (5) is

$$\begin{aligned} &\widetilde{v}(x_i) = \widetilde{H}[\widetilde{v}](x_i), \quad x_i \in (\Omega \backslash \mathcal{C}) \cap G, \\ &\widetilde{v}(x_i) = 0, \quad x_i \in \mathcal{C} \cap G, \end{aligned} \tag{6}$$

where

$$\widetilde{H}[\widetilde{v}](x_i) := \min_{u \in U}\{\mathbb{P}_1(\widetilde{v}; x_i + hf(x_i,u)) + h\ell(x_i,u)(1 - \widetilde{v}(x_i))\} \tag{7}$$

and $\mathbb{P}_1(\widetilde{v}; x_i + hf(x_i,u))$ denotes the value of $\widetilde{v}$ at the point $x_i + hf(x_i,u)$ obtained by linear interpolation (note that the point $x_i + hf(x_i,u)$ is not in general sitting on the grid). The numerical scheme consists in iterating the fixed point sequence

$$\widetilde{v}^{(n+1)} = \widetilde{H}[\widetilde{v}^{(n)}], \quad n = 1, 2, \ldots, \tag{8}$$

until convergence, starting from $\widetilde{v}^{(0)}(x_i) = 0$ on $\mathcal{C}$ and $\widetilde{v}^{(0)}(x_i) = 1$ elsewhere. To speed up the convergence, we use the fast sweeping technique [25]. The function

$\widetilde{v}$ is then extended to the whole space by linear interpolation. Once the function $\widetilde{v}$ is computed, we get easily the corresponding approximation $\widetilde{\mathcal{T}}$ of $\mathcal{T}$ and then the optimal control law in feedback form; see [14, 15] for details.

It is also useful to note that (5) models a front (interface) propagation problem. Following this interpretation, the boundary of the target $\partial\mathcal{C}$ is the front at initial time $t = 0$; the level set $\{x : \mathcal{T}(x) = t\}$ represents the front at any time $t > 0$.

3 Coupling HJB and PMP

3.1 Main Connection

It is known [7] that, for a general control problem with free endpoint, if the value function is differentiable at some point $x \in \mathbb{R}^d$, then it is differentiable along the optimal trajectory starting at x. Actually, *the gradient of the value function is equal to the costate of the Pontryagin principle*. In the context of minimum time problems (with target constraint), the link between the minimum time function and the Pontryagin principle has been also investigated in several papers [8, 9], proving the same connection.

The main idea of the paper is to compute an approximation of the value function $\mathcal{T}$ solving the HJB equation on a rough grid, then approximate $D\mathcal{T}(x)$ (x being the starting point) and finally use it as initial guess for $p(0)$. The approximation of the gradient can be obtained by standard first-order centered finite differences.

In the case $\mathcal{T} \notin C^1(\mathbb{R}^d)$, it is proved in [8] that a connection between the two approaches still exists. More precisely, under some additional assumptions, we have

$$p^*(t) \in D^+\mathcal{T}(y_x^*(t)), \quad t \in [0, \mathcal{T}(x)],$$

where $D^+\mathcal{T}(x)$ is the *superdifferential* of $\mathcal{T}$ at x defined by

$$D^+\mathcal{T}(x) := \left\{ \eta \in \mathbb{R}^d : \limsup_{y \to x} \frac{\mathcal{T}(y) - \mathcal{T}(x) - \eta \cdot (y - x)}{|y - x|} \leq 0 \right\}. \tag{9}$$

In the rest of this section, we assume that $D^+\mathcal{T}(x) \neq \emptyset$. It is plain that we cannot use a finite-difference approximation in order to compute $p(0)$ at the points where the value function $\mathcal{T}$ is not differentiable. Instead, we follow a different strategy. Let $\delta > 0$ be a small positive parameter and let $B(0, 1)$ denote the unit ball in $\mathbb{R}^d$ centered at 0. We first compute the vector

$$\widetilde{\xi}^* := \frac{\mathcal{T}(x + \delta\widetilde{\zeta}^*) - \mathcal{T}(x)}{\delta}\widetilde{\zeta}^*, \tag{10}$$

with

$$\widetilde{\zeta}^* := \arg \min_{\zeta \in B(0,1)} \mathcal{T}(x + \delta\zeta).$$

Note that $\widetilde{\zeta}^*$ is an approximation of the direction of maximal decrease of $\mathcal{T}$ and that $\|\widetilde{\xi}^*\|$ is an approximation of the directional derivative of $\mathcal{T}$ along the direction

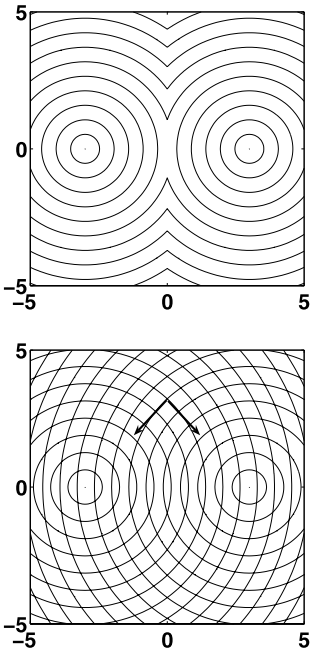

Fig. 1 Two crossing fronts with and without superimposition. *Arrows* correspond to the (two) vector(s) $\widetilde{\zeta}^*$

$\widetilde{\zeta}^*$. Since in the case $\mathcal{T} \in C^1(\mathbb{R}^d)$ the direction $\widetilde{\xi}^*$ is a first-order approximation of $D\mathcal{T}(x)$, we use $\widetilde{\xi}^*$ as the initial guess for the costate $p(0)$.

Let us explain on a simple example why we choose the definition (10). Consider the case

$$d = 2, \qquad \mathcal{C} = \{(3,0)\} \cup \{(-3,0)\}, \qquad \ell \equiv 1, \qquad f = u, \qquad U = B(0,1).$$

In this case, the HJB equation reduces to the eikonal equation $\|D\mathcal{T}(x)\| = 1$. On the line $\{x = 0\}$, the function $\mathcal{T}$ is not differentiable; see the level sets in Fig. 1(top). This line corresponds to a zone where two optimal trajectories are available, i.e. the functional J has two global minima. Following the front propagation interpretation (see the end of Sect. 2.2), here we have two fronts which hit each other at the line $\{x = 0\}$. The viscosity solution of the HJB equation selects automatically the first arrival time, so we never see the two crossing fronts, but we could in principle follow the propagations of the two fronts separately (Fig. 1(bottom)) and then compute the two gradients of the two value functions. These two gradients correspond to the two optimal choices for $p(0)$. By means of (10), we can approximate the two gradients without splitting the evolutions of the fronts. We first compute the two directions $\widetilde{\zeta}_1^*$, $\widetilde{\zeta}_2^*$ of maximal decrease of the function $\mathcal{T}$ (Fig. 1(bottom)) and then the two gradients $\widetilde{\xi}_1^*$, $\widetilde{\xi}_2^*$ of $\mathcal{T}$.

In the present example, focusing on the point $(0,0)$, the two directions of maximal decrease are $(-1,0)$ and $(1,0)$. It is easy to show that these two vectors coincide with the two extremal vectors in $D^+\mathcal{T}(x)$, namely the vectors η verifying

$$\limsup_{y \to x} \frac{\mathcal{T}(y) - \mathcal{T}(x) - \eta \cdot (y - x)}{|y - x|} = 0. \tag{11}$$

Although this relationship is not true for every function $\mathcal{T}$ such that $D^+\mathcal{T}(x) \neq \emptyset$, it is easy to see that it is true whenever the curve of nondifferentiability is due to the collision of two or more fronts (as in P1, Sect. 5).

In Sect. 4, we show that, beside an initial guess for $p(0)$, also other useful data can be extrapolated from the value function and used to start the shooting method.

3.2 Convergence of $D\mathcal{T}$

Let us denote by $\widetilde{D} = (\widetilde{D}_1, \ldots, \widetilde{D}_d)$ the discrete gradient computed by centered finite differences with step $z > 0$,

$$\widetilde{D}_i \mathcal{T}(x) := \frac{\mathcal{T}(x + ze_i) - \mathcal{T}(x - ze_i)}{2z}, \quad i = 1, \ldots, d,$$

where $\{e_i\}_{i=1,\ldots,d}$ is the standard basis of $\mathbb{R}^d$.

Many papers (see for example [26, 27] in the context of differential games) investigated the convergence of the approximate value function $\widetilde{v}(\cdot; h, k, \Omega)$ to the exact solution v when the parameters h, k tend to zero and Ω tends to $\mathbb{R}^d$. These results were quite difficult to be obtained, because the function v is not in general differentiable. For our purposes, we have to go farther, proving the convergence of $\widetilde{\mathcal{T}}(\cdot; h, k, \Omega) = -\log(1 - \widetilde{v}(\cdot; h, k, \Omega))$ to $\mathcal{T}$ and then the convergence of $\widetilde{D}\widetilde{\mathcal{T}}(\cdot; h, k, z, \Omega)$ to $D\mathcal{T}$, because the latter is used by the PMP method as initial guess.

Let us assume that $k = C_1 h$ for some positive constant C_1. Given a generic estimate of the form

$$\|\widetilde{v}(\cdot; h, \mathbb{R}^d) - v(\cdot)\|_{L^\infty(\mathbb{R}^d)} \leq Ch^\alpha, \quad C, \alpha > 0, \tag{12}$$

we have the following theorem.

Theorem 3.1 *Let Ω be a subset of $\mathbb{R}^d$ such that $\mathcal{C} \subset \Omega$. Assume that $\mathcal{T} \in C^1(\Omega)$ and that there exists $\mathcal{T}_{\max} > 0$ such that*

$$0 \leq \mathcal{T}(x) \leq \mathcal{T}_{\max}, \quad \textit{for all } x \in \Omega.$$

Let us define

$$E(x; h, z, \Omega) := \|\widetilde{D}\widetilde{\mathcal{T}}(x; h, z, \Omega) - D\mathcal{T}(x)\|_\infty,$$

where $\|\ \|_\infty$ is the maximum norm in $\mathbb{R}^d$.

Then, there exists $\Omega' \subset \Omega$ such that

$$\|E(\cdot; h, z, \Omega)\|_{L^\infty(\Omega')} = O(h^\alpha/z) + O(z^2), \quad h, z \to 0.$$

For the SL scheme, an estimate of the form (12) in the particular case $\ell \equiv 1$ (under assumptions weaker than those used in Theorem 3.1) can be found in [27]. The proof of the theorem is postponed to the Appendix.

4 Numerical Experiments

We have tested the feasibility and relevance of combining the HJB and PMP methods on four optimal control problems. Each of these problems highlights a particular difficulty from the control point of view.

Problem P1 (Sect. 5) is a two-dimensional minimum time target problem with local and global minima. We see in this example that the shooting method is very sensitive with respect to the initial guess (as usual).

Problem P2 (Sect. 6) is a two-dimensional controlled Van der Pol oscillator with control switchings.

Problem P3 (Sect. 7) is the well-known Goddard problem with singular arcs, in the one-dimensional case (total state dimension is three).

Problem P4 (Sect. 8) is another minimum time target problem in dimension four, with a first-order state constraint.

4.1 Details for the HJB Implementation

The algorithm is written in C++ and ran on a PC with an Intel Core 2 Duo processor at 2.00 GHz and 4 GB RAM. The code is not parallelized. The reported CPU time is the time required for the whole process, which includes computing the value function, its gradient, the optimal trajectory and saving the results on file.

The grid G has $N_1 \times \cdots \times N_d$ nodes. Grid cells have the same size k in any dimension. The set of admissible controls U is discretized in N_C equispaced discrete controls $\{u_j,\ j = 1, \ldots, N_C\}$. The (fictitious) time step h is variable, and chosen in such a way that $h|f(x_i, u_j)| = k$ for any x_i and u_j, so that the stencil is limited to the eight neighbouring nodes (plus the considered node itself). The stop criterion for the fixed point iterations (8) is $\|\widetilde{v}^{(n+1)} - \widetilde{v}^{(n)}\|_{L^\infty(\Omega)} < \varepsilon = 10^{-5}$.

4.2 Details for PMP Implementation

The algorithm is written in Fortran 90 and ran on a PC with an Intel Core 2 Duo processor at 2.33 GHz and 2 GB RAM. We use the SHOOT[1] software which implements a shooting method with the HYBRD [28] solver. For the four problems studied, we set the ODE integration method to a basic 4th order Runge-Kutta with 100 steps.

Discretization parameters and CPU times for all the numerical tests are summarized in Sect. 9.

5 Minimum Time Target Problem

The first example illustrates how a local solution can affect the shooting method. We consider a simple minimum time problem in two dimensions. The goal is to reach a given position on the plane in minimum time. The control is the direction of the

[1] http://www.cmap.polytechnique.fr/~martinon/.

velocity. We choose the velocity in such a way that the cost functional has multiple minima.

$$
\begin{aligned}
\text{(P1)} \qquad \min \quad & t_f, \\
\text{s.t.} \quad & \dot{y}_1(t) = c(y_1(t), y_2(t)) \cos(u(t)), \\
& \dot{y}_2(t) = c(y_1(t), y_2(t)) \sin(u(t)), \\
& U = [0, 2\pi), \\
& y(0) = x = (-2.5, 0), \\
& y(t_f) = (3, 0),
\end{aligned}
$$

with

$$
c(y_1, y_2) = \begin{cases} 1, & \text{if } y_2 \leq 1, \\ (y_2 - 1)^2 + 1, & \text{if } y_2 > 1. \end{cases}
$$

5.1 PMP and Shooting Method

We first try to solve the problem with the PMP and the shooting method. Therefore, we seek the zero of the shooting function defined by

$$
S_1 : \begin{pmatrix} t_f \\ p_1(0) \\ p_2(0) \end{pmatrix} \mapsto \begin{pmatrix} y_1(t_f) - 3 \\ y_2(t_f) \\ p_3(t_f) - 1 \end{pmatrix}.
$$

Depending on the initial guess, the shooting method can converge to a local or global solution (Fig. 2). The most common local solution is the straight line trajectory $(-)$ from x to $\mathcal{C} := \{(3, 0)\}$, with a constant control $u = 0$ and a final time $t_f = 5.5$. The global solution has an arch shaped trajectory $(\cap)$ that benefits from the higher speed for increasing values of y_2, with a final time $t_f^* = 4.868$.

Even for this simple problem, the shooting method is very sensitive to the starting point. Numerical tests indicate that it converges in most cases to local solutions. We ran the shooting method with a batch of 441 values for $p(0)$, equally distributed in $[-10, 10]^2$, and for two different starting guesses for the final time (Fig. 3). We observe that, for the batch with the $t_f = 1$ initialization, 11% of the shootings converge to the global solution, 60% to the straight line local solution, and 24% to another local solution with an even worse final time ($t_f = 6.06$). The remaining 5% does not converge at all. For the batch with the $t_f = 10$ initialization, 9% of the shootings converge to the global solution, 50% and 29% to the two local solutions, and 12% does not converge. Obviously, just taking a random starting point is not a reliable way to find the global solution.

5.2 Solving the Problem with the HJB Approach

In Fig. 4, we show the level sets of the minimum time function $\mathcal{T}$ associated to the control problem (P1). The numerical domain is $\Omega = [-6, 6]^2$. The optimal trajecto-

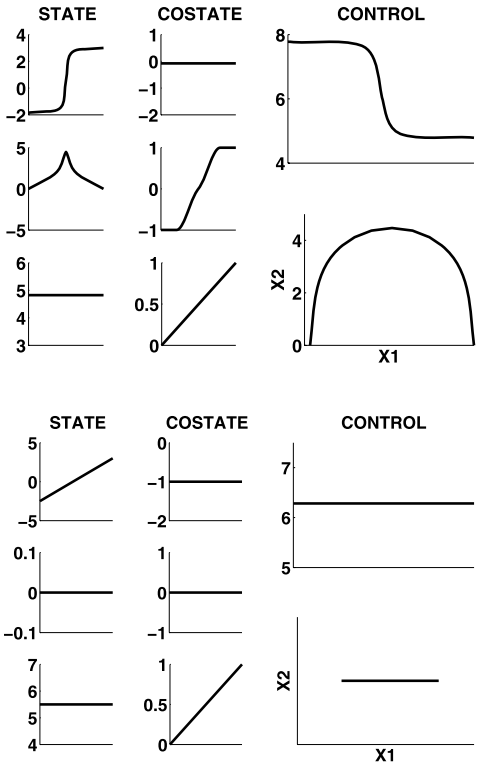

Fig. 2 (P1) Global solution (*curved trajectory*) and local solution (*straight trajectory*) found by the shooting method. Control must be intended modulo 2π

ries to the target are the curves orthogonal to the level sets. Local solutions cannot be recovered.

As it can be seen, the minimum time function is not differentiable everywhere. The curve of nondifferentiability represents here the set of the points where two optimal trajectories are available. The superdifferential $D^+\mathcal{T}$ at the points of nondifferentiability is nonempty. Notice that here the minimum time function remains differentiable along each trajectory. We will see in Sect. 6 a different type of nondifferentiability for the value function.

5.3 Coupling the HJB and PMP Approaches

We now use the data provided by the HJB approach to obtain a starting point close to the global solution. The HJB solution provides not only an approximation of the costate $p(0)$, but also an estimate of the optimal final time t_f^*. In Table 1, we summarize the results obtained by solving the HJB equation on several grids. As we can see, the outcome is not very sensitive with respect to the discretization parameters. This means that the choice of a very rough grid can be sufficient to obtain a good initial guess for PMP. In fact, the shooting method converges immediately to the global solution when using the starting point obtained by the HJB method on the coarsest grid (Table 2).

We can check that the convergence of the shooting method is much easier in a neighbourhood of the HJB initialization. We test again a batch of 441 values for $p(0)$,

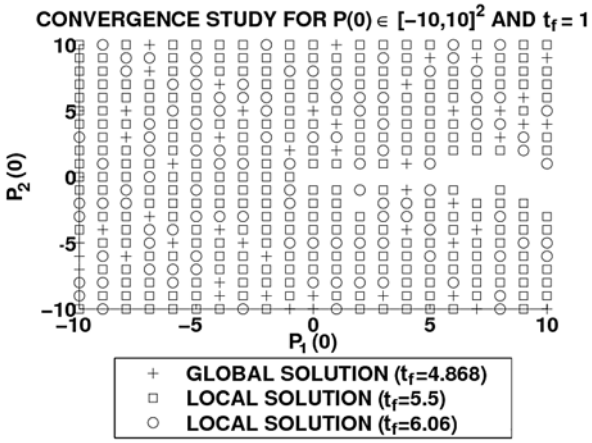

Fig. 3 (P1) Convergence from a random initialization

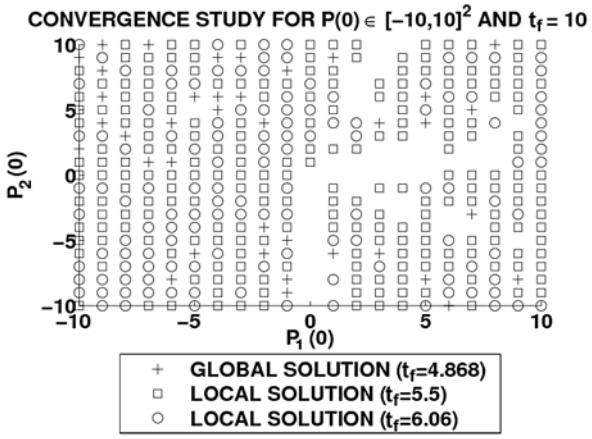

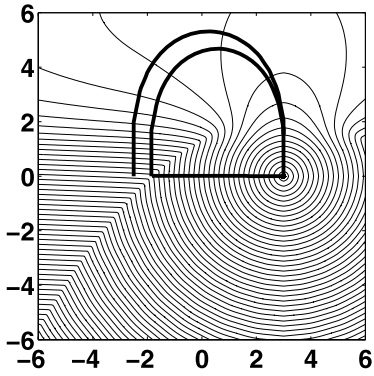

Fig. 4 (P1) Level sets of the minimum time function $\mathcal{T}$, the optimal trajectory starting from $(-2.5, 0)$ and the two optimal trajectories starting from $(-1.835, 0)$

equally distributed in $[-0.1, 0] \times [-2, 0]$, which corresponds to a 100% range around the HJB initialization $(-0.05, -1)$. We also set $t_f = 4.89$. This time the shooting

Table 1 (P1) HJB approach: minimal time and initial costate associated to the optimal trajectory

$N_1 \times N_2$	N_C	t_f^*	$p(0)$	CPU time (sec)
25×25	16	4.895	$(-0.049, -1.000)$	0.08
50×50	16	4.895	$(-0.048, -1.000)$	0.37
200×200	32	4.878	$(-0.051, -1.000)$	20.25

Table 2 (P1) Initialization by HJB and solution by PMP

	t_f^*	$p(0)$
Initialization by HJB	4.89	$(-0.05, -1)$
Solution by PMP	4.868	$(-5.552 \times 10^{-2}, -9.985 \times 10^{-1})$

Table 3 (P1) Initialization by HJB and solution by PMP (two global solutions)

	t_f^*	$p(0)$
Initialization by HJB ($\cap$)	4.84	$(-0.05, -1)$
Solution by PMP ($\cap$)	4.8246	$(-7.67 \times 10^{-2}, -9.97 \times 10^{-1})$
Initialization by HJB $(-)$	4.84	$(-0.99, 0)$
Solution by PMP $(-)$	4.835	$(-1, -6.2137 \times 10^{-16})$

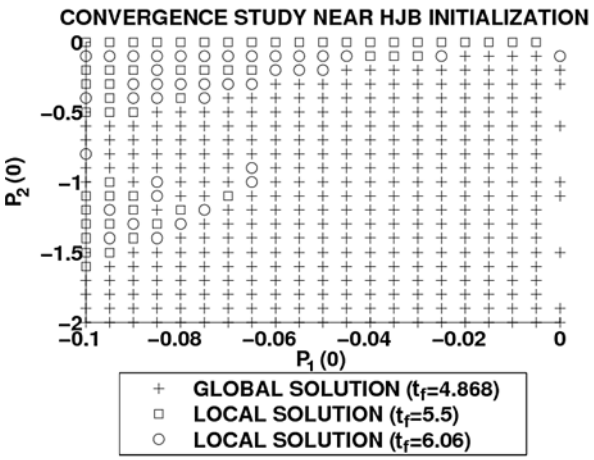

Fig. 5 (P1) Convergence to the global solution is much easier near the HJB initialization

method finds the global solution for 76% of the starting points, and local solutions for only 12% and 9% of the starting points (Fig. 5).

We also consider the case of a starting point very close to the curve where the minimum time function is not differentiable: $x = (-1.835, 0)$. The HJB equation is solved on a 300×300 grid with $N_C = 32$. The two optimal trajectories are shown in Fig. 4. Here the approximation of $p(0)$ (see Sect. 3.1) gives the two directions

$p_1(0) = (-0.05, -1.00)$ and $p_2(0) = (-0.99, 0.00)$. Using these two values to initialize the shooting method, we obtain the two distinct solutions with the "cap" and "straight" trajectories (Table 3).

6 Van der Pol Oscillator

The second test problem is a controlled Van der Pol oscillator. Here we want to reach the steady state $(y_1, y_2) = (0, 0)$ in minimum time. It is well known that the optimal trajectories for this problem are associated with bang-bang control variables.

$$
\begin{aligned}
\text{(P2)} \quad \min \quad & t_f, \\
\text{s.t.} \quad & \dot{y}_1(t) = y_2(t), \\
& \dot{y}_2(t) = -y_1(t) + y_2(t)(1 - y_1(t)^2) + u(t), \\
& U = [-1, 1], \\
& y(0) = x = (1, -0.8), \\
& y(t_f) = (0, 0).
\end{aligned}
$$

6.1 PMP and Shooting Method

Here, the Hamiltonian is linear with respect to u. Therefore, we have a bang-bang control with the switching function $\psi(y, p) = H_u(y, p, u) = p_2$. The shooting function is defined by

$$
S_2 : \begin{pmatrix} t_f \\ p_1(0) \\ p_2(0) \end{pmatrix} \mapsto \begin{pmatrix} y_1(t_f) \\ y_2(t_f) \\ p_3(t_f) - 1 \end{pmatrix}.
$$

We test the shooting method with the same initial points as for problem (P1). The convergence results are even worse in this case: for the $t_f = 1$ initialization, only 9% of the shootings converge to the global solution; for the $t_f = 10$ initialization, only 0.5% of the shootings converge to the global solution.

6.2 Solving the Problem with the HJB Approach

Here, we use the HJB approach to compute the minimum time function. In Fig. 6, we show the level sets of the solution obtained in $\Omega = [-2, 2]^2$ and the optimal trajectory starting from $(1, -0.8)$. As in the previous problem, the value function is not differentiable everywhere, but here the curve of nondifferentiability has a different nature. It can no more be seen as the curve of collision between two fronts and is not caused by the existence of multiple optimal solutions. It corresponds to the points where the control switches between -1 and $+1$. Taking such starting points, we have a solution with constant control $u = \pm 1$ and no switches. Finally, we observe that, at the points of nondifferentiability, the superdifferential is empty.

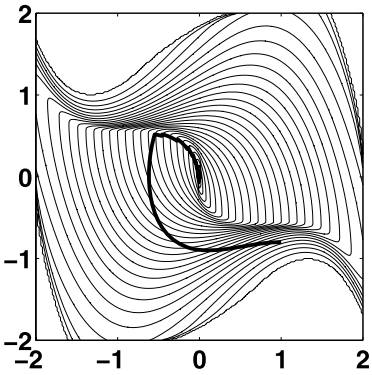

Fig. 6 (P2) Level sets of function $\mathcal{T}$ and the optimal trajectory starting from $(1, -0.8)$

Table 4 (P2) Initialization by HJB and solution by PMP

	t_f^*	$p(0)$
Initialization by HJB	4.2	$(1.2, -4.2)$
Solution by PMP	3.837	$(1.249, -3.787)$

6.3 Coupling the HJB and PMP Approaches

As before, the numerical solution of the HJB equation provides an approximation of the final time t_f and an initial costate $p(0)$. This information is used here to start the shooting algorithm. Once again, the HJB initialization gives an immediate accurate convergence to the optimal solution; see Table 4 and Fig. 7. In this example, the control discontinuities hinder the convergence by testing different integration schemes for the state and costate pair (y, p). Using a fixed step integrator (4th order Runge-Kutta) without any precaution gives a very poor convergence with a norm of $\approx 10^{-3}$ for the shooting function. Using either a variable step integrator (DOPRI [29]) or a switching detection method for the fixed-step integrator [30], we get much better results ($\approx 10^{-11}$ for the shooting function norm).

We now test two other starting points positioned very close to the curve where the value function is not differentiable, namely $x = (1.5, -0.67)$ and $x = (1, -0.57)$. Computation of the gradient is performed as described in Sect. 3.1 in the case where $\mathcal{T}$ is not differentiable, even if here that method is not in principle applicable due to the different nature of the nondifferentiability. We observe that the shooting method finds solutions with a switch immediately after the initial time or just before the final time. Here, the initial guesses for the costate $p(0)$ provided by the HJB method are not so close to the right ones, but they are sufficient to obtain convergence. Conversely, the minimum times given by HJB are rather close to the exact ones (Table 5).

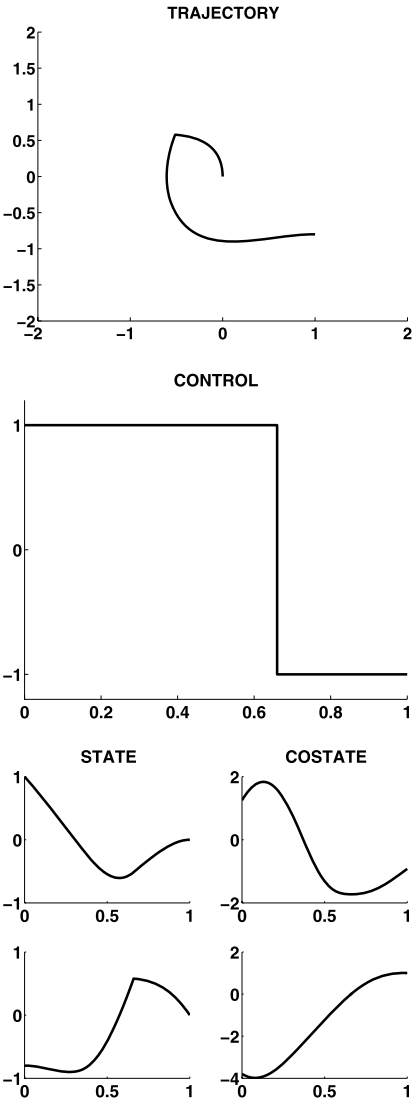

Fig. 7 (P2) Solution with one switch for the Van der Pol oscillator (shooting method)

Table 5 (P2) Initializations by HJB and solutions by PMP, nondifferentiable case

	t_f^*	$p(0)$
Init. by HJB ($x = (1.5, -0.67)$)	3.0	$(1.62, -0.87)$
Sol. by PMP ($x = (1.5, -0.67)$)	2.9594	$(1.487, 2.309 \times 10^{-3})$
Init. by HJB ($x = (1, -0.57)$)	2.2	$(1.96, -0.10)$
Sol. by PMP ($x = (1, -0.57)$)	2.1351	$(1.715, 1.111 \times 10^{-2})$

7 Goddard Problem

The third example is the well-known Goddard problem (see for instance [31–36], to illustrate the case of singular arcs. This problem models the ascent of a rocket through the atmosphere. We restrict ourselves to vertical (monodimensional) trajectories: the state variables are the altitude, velocity and mass of the rocket during the flight, so we have $d = 3$. The rocket is subject to gravity, thrust (controlled) and drag forces. The final time is free and the objective is to reach a certain altitude with minimal fuel consumption,

$$
\begin{aligned}
\text{(P3)} \quad \min \quad & \int_0^{t_f} b\, T_{\max}\, u(t)\, dt, \\
\text{s.t.} \quad & \dot r = v, \\
& \dot v = -\frac{1}{r^2} + \frac{1}{m}(T_{\max} u - D(r, v)), \\
& \dot m = -b\, T_{\max}\, u, \\
& U = [0, 1], \\
& r(0) = 1,\ v(0) = 0,\ m(0) = 1, \\
& r(t_f) \geq 1.01,
\end{aligned}
$$

with the parameters used for instance in [33]: $b = 2$, $T_{\max} = 3.5$, drag $D(r, v) = 310 v^2 e^{-500(r-1)}$.

7.1 PMP and Shooting Method

As for (P2), the Hamiltonian is linear with respect to u and we have a bang-bang control with possible switchings or singular arcs. The switching function is

$$
\psi(y, p) = H_u(y, p, u) = T_{\max}\left((1 - p_m)b + \frac{p_v}{m}\right)
$$

and the singular control can be obtained by formally solving $\ddot\psi = 0$. The main difficulty, however, is to determine the structure of the optimal control, namely the number and approximate location of the singular arcs. The HJB approach is able to provide such information, in addition to the initial costate $p(0)$ and optimal time t_f^*. Assuming for instance one interior singular arc, the shooting function is defined by

$$
S_3 : \begin{pmatrix} t_f, p_1(0), p_2(0), p_3(0) \\ t_{\text{entry}} \\ t_{\text{exit}} \end{pmatrix} \mapsto \begin{pmatrix} r(t_f) - 1.01, p_2(t_f), p_3(t_f), p_4(t_f) \\ \psi(y(t_{\text{entry}}), p(t_{\text{entry}})) \\ \dot\psi(y(t_{\text{entry}}), p(t_{\text{entry}})) \end{pmatrix}.
$$

7.2 Solving the Problem with the HJB Approach

The Goddard problem is also hard to solve with the HJB approach, especially because the computation of the value function needs a huge number of iterations to converge

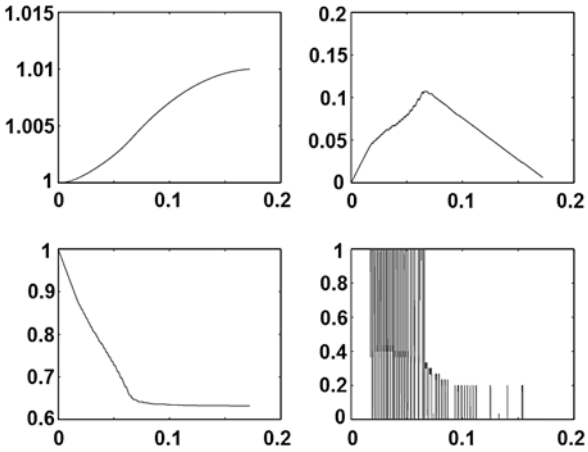

Fig. 8 (P3) Goddard problem, solution by the HJB approach (*first line*: altitude and velocity. *Second line*: mass and control)

Table 6 (P3) Initialization by HJB and solution by PMP

	t_f^*	$(t_{\text{entry}}, t_{\text{exit}})$	$p(0)$
Init. by HJB	0.17	(0.02, 0.06)	(−7.79, −0.31, 0.04)
Sol. by PMP	0.1741	(0.02351, 0.06685)	(−7.275, −0.2773, 0.04382)

and the solution is quite sensitive to the choice of the numerical box Ω in which the value function is computed. In Fig. 8, we show the optimal trajectory and the optimal control computed via HJB in $\Omega = [0.998, 1.012] \times [-0.02, 0.18] \times [0.1, 1.8]$. As we can see, the HJB approach does not give a good approximation of the optimal control (vertical lines correspond to strong oscillations of the solution).

7.3 Coupling the HJB and PMP Approaches

As for problems (P1) and (P2), for problem (P3) the HJB solution provides an estimate of the final time t_f^* and initial costate $p(0)$. Moreover, an examination of the HJB solution gives a good idea of the structure of the optimal control and the optimal trajectory: the change of slope on the velocity clearly visible in Fig. 8 indicates an interior singular arc at $(t_{\text{entry}}, t_{\text{exit}}) \approx (0.02, 0.06)$. The same information can be deduced by the optimal control, strongly oscillating in the same time interval. Initializing the shooting method by means of these rough guesses, once again we obtain quick convergence to the correct solution with the expected singular arc (Table 6 and Fig. 9).

8 Minimum Time Target Problem with a State Constraint

This fourth example aims at illustrating the case of a state constraint as well as a four-dimensional problem for the HJB approach. The goal is to move a point on a plane, from an initial position to a target position, with null initial and final velocity.

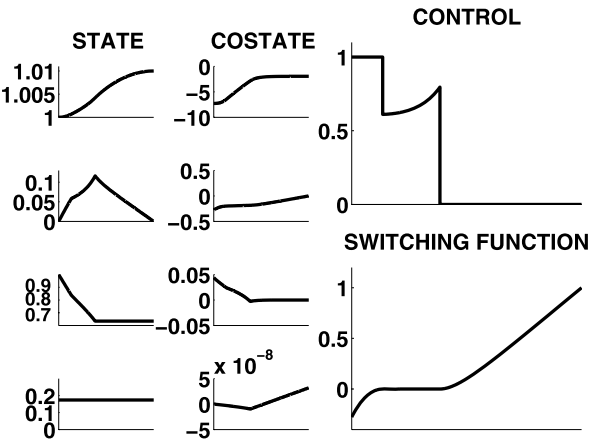

Fig. 9 (P3) Goddard problem, solution by the PMP method

The control is the direction of the acceleration and the objective is to minimize the final time. We add a state constraint, which limits the velocity along the x-axis. The problem is as follows:

$$
\begin{aligned}
\text{(P4)} \quad \min \quad & t_f, \\
\text{s.t.} \quad & \dot{y}_1(t) = y_3(t), \\
& \dot{y}_2(t) = y_4(t), \\
& \dot{y}_3(t) = \cos(u(t)), \\
& \dot{y}_4(t) = \sin(u(t)), \\
& U = [0, 2\pi), \\
& y(0) = x = (-3, -4, 0, 0), \\
& y(t_f) = (3, 4, 0, 0), \\
& y_3(t) \leq 1, \quad t \in (0, t_f).
\end{aligned}
$$

Let us write the state constraint as $g(y(t)) \leq 0$, with g defined by $g(y) = y_3 - 1$. The control appears explicitly in the first time derivative of g, so the constraint is of order 1, and we have

$$\dot{g}(y(t)) = \cos(u(t)), \quad g_y(y) = (0, 0, 1, 0).$$

When the constraint is not active, minimizing the Hamiltonian gives the optimal control u^* via

$$(\cos(u^*), \sin(u^*)) = -\frac{(p_3, p_4)}{\sqrt{p_3^2 + p_4^2}}.$$

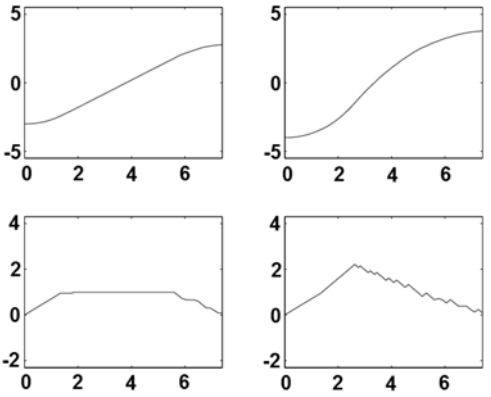

Fig. 10 (P4) Solution with a constrained arc by the HJB approach (*first line*: the two components $y_1(t)$ and $y_2(t)$ of the space. *Second line*: the two components $y_3(t)$ and $y_4(t)$ of the velocity)

Over a constrained arc where $g(y) = 0$, the equation $\dot{g}(y, u) = 0$ and minimizing the Hamiltonian H leads to

$$u^* = -\text{sign}(p_4)\frac{\pi}{2}.$$

Then the condition $H_u = 0$ gives the value for the constraint multiplier $\mu = -p_3$. At the entry point, we have a jump condition for the costate,

$$p(t^+_{\text{entry}}) = p(t^-_{\text{entry}}) - \pi_{\text{entry}}\ g_y,$$

with $\pi_{\text{entry}} \in \mathbb{R}$ an additional shooting unknown. Compared to the unconstrained problem, we have three more unknowns $t_{\text{entry}}, t_{\text{exit}}, \pi_{\text{entry}}$. The corresponding equations are the Hamiltonian continuity at t_{entry} and t_{exit} (which boils down to $p_3 = 0$) and the tangential entry condition $g(y(t_{\text{entry}})) = 0$. The shooting function is defined by

$$S_4 : \begin{pmatrix} t_f \\ p_{1\ldots4}(0) \\ t_{\text{entry}}, t_{\text{exit}}, \pi_{\text{entry}} \end{pmatrix} \mapsto \begin{pmatrix} p_5(t_f) - 1 \\ y_{1\ldots4}(t_f) - (-3, -4, 0, 0) \\ p_3(t_{\text{entry}}),\ p_4(t_{\text{entry}}),\ g(y(t_{\text{entry}})) \end{pmatrix}.$$

In Fig. 10, we show the numerical solution obtained by using the HJB approach in $[-5, 5]^2 \times [-2, 4]^2$. In addition to the optimal final time and the initial costate, the HJB solution gives an estimate of the bounds for the constrained arc where $y_3 = 1$. The only shooting unknown for which we were not able to obtain relevant information is the multiplier π_{entry} for the costate jump at t_{entry}. Therefore, we used $\pi_{\text{entry}} = 0.1$ as a starting guess, which turned out to be sufficient for the shooting method to converge properly (Table 7). Figure 11 shows the corresponding solution, much cleaner than the HJB solution, but with the same structure. We checked that the condition $\mu \geq 0$ was satisfied over the boundary arc as p_3 is negative and $p_3 = 0$ at both entry and exit of the arc as requested by the Hamiltonian continuity conditions. The actual value of the multiplier for the jump on p_3 is $\pi_{\text{entry}} = 4.1294$.

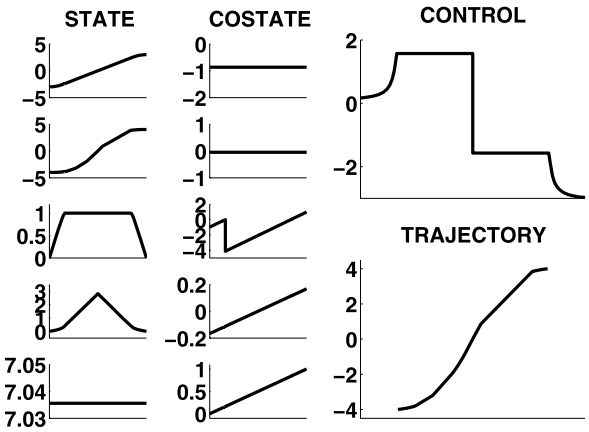

Fig. 11 (P4) Solution with a constrained arc by the PMP approach

Table 7 (P4) Initialization by HJB and solution by PMP

	t_f^*	$(t_{\text{entry}}, t_{\text{exit}})$	$p(0)$
Init. by HJB	7.5	(1.35, 5.6)	(−0.51, −0.24, −0.89, −0.61)
Sol. by PMP	7.0356	(1.137, 5.899)	(−0.867, −0.047, −0.986, −0.167)

Table 8 Summary of discretization parameters for HJB

	P1	P2	P3	P4
$N_1 \times \cdots \times N_d$	25×25	200×200	$20 \times 20 \times 20$	$20 \times 20 \times 20 \times 20$
N_C	16	2	20	16

Table 9 Summary of CPU times (seconds) and shooting function norm

	P1	P2	P3	P4
HJB	8×10^{-2}	2.98	211	182
PMP	3×10^{-3}	7×10^{-3}	3×10^{-2}	2×10^{-2}
$\|S\|$	2.82×10^{-16}	8.14×10^{-11}	1.12×10^{-7}	6.68×10^{-11}

9 Discretization Parameters and CPU Times

In Table 8, we report the discretization parameters for HJB used in the four numerical tests. Note that the Van der Pol problem needs a rather fine grid to obtain a sufficient accuracy. In Table 9, we report the CPU times and the norm of the shooting function at the end of the computations. The large time for the Goddard problem is due to the huge number of iteration needed by the HJB approach.

10 Conclusions and Future Work

The known relation between the gradient of the value function in the HJB approach and the costate in the PMP approach allows to use the HJB results to initialize a shooting method. With this combined method, one can hope to benefit from the optimality of HJB and the high precision of PMP.

We have tested the combined approach on four control problems presenting some specific difficulties. The numerical tests also included two cases where the value function is not differentiable. For these four problems, the HJB approach provides useful data such as an estimate of the initial costate $p(0)$, the optimal final time t_f^*, and the structure of the optimal solution with respect to singular or constrained subarcs. In each case, this information allowed us to successfully initialize the shooting method. The fact that the optimal control computed by HJB is sometimes far from the exact control did not seem to be a main issue for the shooting method initialization. The total computational time for the combined HJB-PMP approach did not exceed four minutes, up to dimension four. This probably allows us to run experiments in higher dimensions, like five or six. Moreover, the code for the HJB equation is easy parallelizable [37].

Even if the main limitation of the proposed method appears to be the state dimension (imposed by HJB), this does not mean that only simple problems can be solved. We plan to apply this approach more specifically to trajectory optimization for space launchers: these problems are still hard despite having a low dimension, typically 3/4 for coplanar flight and 5/6 for 3D flight. Experiments are in progress for the Ariane 5 launcher (mission toward a GTO orbit) and for a prototype of a reusable launcher with wings (toward a LEO orbit).

Acknowledgements The authors thank Hasnaa Zidani for proposing the main idea of the paper and for suggestions.

Appendix

Proof of Theorem 3.1 Given the numerical domain Ω, we define the set Ω' as

$$\Omega' := \left\{ x \in \mathbb{R}^d : \widetilde{v}(x; h, \Omega) \leq \min_{x' \in \partial\Omega} \widetilde{v}(x'; h, \Omega) \right\}.$$

The set Ω is the box in which the approximate solution is actually computed and Ω' represents the subset of Ω in which the solution is not affected by the fictitious boundary conditions we need to impose at $\partial\Omega$ to make computation. From the front propagation point of view, $\partial\Omega'$ represents the front at the time it touches $\partial\Omega$ for the very first time.

Let us define $v_{\max} := (1 - e^{-\mathcal{T}_{\max}})$ and fix $x \in \Omega'$. We have

$$\mathcal{T}(x) \leq \mathcal{T}_{\max} < +\infty \quad \text{and} \quad v(x) \leq v_{\max} < 1.$$

By (12), we have

$$\widetilde{v}(x; h) \leq v(x) + Ch^{\alpha} \leq v_{\max} + Ch^{\alpha}.$$

Since $v_{\max} < 1$, there exists $h_0 > 0$ such that

$$v_{\max} + Ch^{\alpha} < 1, \quad \text{for all } 0 < h \le h_0$$

then we can define

$$\widetilde{v}_{\max} := v_{\max} + Ch_0^{\alpha} < 1$$

and we have

$$v(x) \le v_{\max} \le \widetilde{v}_{\max} \quad \text{and} \quad \widetilde{v}(x;h) \le \widetilde{v}_{\max} \quad \text{for all } x \in \Omega',\ 0 < h \le h_0.$$

For any fixed $x \in \Omega'$, there exists $\xi_x \in [\min\{v(x), \widetilde{v}(x;h)\}, \max\{v(x), \widetilde{v}(x;h)\}]$ such that

$$|\widetilde{\mathcal{T}}(x) - \mathcal{T}(x)| = \left|\log\big(1 - v(x)\big) - \log\big(1 - \widetilde{v}(x;h)\big)\right| = \left|\frac{1}{1-\xi_x}\right| |v(x) - \widetilde{v}(x;h)|.$$

Since $\xi_x \le \widetilde{v}_{\max}$, we have

$$|\widetilde{\mathcal{T}}(x) - \mathcal{T}(x)| \le \frac{Ch^{\alpha}}{1 - \widetilde{v}_{\max}}, \quad \text{for all } x \in \Omega' \text{ and } 0 < h \le h_0$$

and then there exists a positive constant C_2 which depends by the problem's data and on Ω such that

$$\|\widetilde{\mathcal{T}} - \mathcal{T}\|_{L^{\infty}(\Omega')} \le C_2 h^{\alpha}, \quad \text{for all } 0 < h \le h_0. \tag{13}$$

We are now ready to recover an estimate on the gradient of the approximate solution $\widetilde{\mathcal{T}}$. By (13), we know that, for any $i = 1, \dots, d$,

$$\widetilde{\mathcal{T}}(x + ze_i) = \mathcal{T}(x + ze_i) + E_1, \quad \text{with } |E_1| \le C_2 h^{\alpha},$$

and

$$\widetilde{\mathcal{T}}(x - ze_i) = \mathcal{T}(x - ze_i) + E_2, \quad \text{with } |E_2| \le C_2 h^{\alpha}.$$

So we have

$$\widetilde{D}_i \widetilde{\mathcal{T}}(x) = \frac{\mathcal{T}(x + ze_i) + E_1 - (\mathcal{T}(x - ze_i) + E_2)}{2z} = \widetilde{D}_i \mathcal{T}(x) + \frac{E_1 - E_2}{2z},$$

so that

$$|\widetilde{D}_i \widetilde{\mathcal{T}}(x) - \widetilde{D}_i \mathcal{T}(x)| \le \left|\frac{E_1 - E_2}{2z}\right| \le C_2 \frac{h^{\alpha}}{z}$$

and then

$$\|\widetilde{D}\widetilde{\mathcal{T}}(x) - \widetilde{D}\mathcal{T}(x)\|_{\infty} \le C_2 \frac{h^{\alpha}}{z}.$$

We finally obtain, for $x \in \Omega'$ and $0 < h \le h_0$,

$$\|\widetilde{D}\widetilde{\mathcal{T}}(x) - D\mathcal{T}(x)\|_{\infty} \le \|\widetilde{D}\widetilde{\mathcal{T}}(x) - \widetilde{D}\mathcal{T}(x)\|_{\infty} + \|\widetilde{D}\mathcal{T}(x) - D\mathcal{T}(x)\|_{\infty}$$

$$= O\left(\frac{h^{\alpha}}{z}\right) + O(z^2)$$

and the conclusion follows. □

References

1. Büskens, C.: NUDOCCCS—User's manual. Universität Münster (1996)
2. Diehl, M., Leineweber, D.B., Schäfer, A.A.S.: MUSCOD-II Users' Manual. University of Heidelberg, Germany (2001)
3. Wächter, A., Biegler, L.T.: On the implementation of a primal-dual interior point filter line search algorithm for large-scale nonlinear programming. Math. Program. **106**, 25–57 (2006)
4. Chudej, K., Büskens, Ch., Graf, T.: Solution of a hard flight path optimization problem by different optimization codes. In: Breuer, M., Durst, F., Zenger, C. (eds.) High-Performance Scientific and Engineering Computing. Lecture Notes in Computational Science and Engineering, vol. 21, pp. 289–296. Springer, New York (2002)
5. Maurer, H., Pesch, H.J.: Direct optimization methods for solving a complex state-constrained optimal control problem in microeconomics. Appl. Math. Comput. **204**, 568–579 (2008)
6. Clarke, F., Vinter, R.B.: The relationship between the maximum principle and dynamic programming. SIAM J. Control Optim. **25**, 1291–1311 (1987)
7. Cannarsa, P., Frankowska, H.: Some characterizations of optimal trajectories in control theory. SIAM J. Control Optim. **28**, 1322–1347 (1991)
8. Cannarsa, P., Frankowska, H., Sinestrari, C.: Optimality conditions and synthesis for the minimum time problem. Set-Valued Anal. **8**, 127–148 (2000)
9. Cernea, A., Frankowska, H.: A connection between the maximum principle and dynamic programming for constrained control problems. SIAM J. Control Optim. **44**, 673–703 (2006)
10. Pesch, H.J.: A practical guide to the solution of real-life optimal control problems. Control Cybern. **23**, 7–60 (1994)
11. Pesch, H.J., Plail, M.: The maximum principle of optimal control: a history of ingenious idea and missed opportunities. Control and Cybern. (to appear)
12. Deuflhard, P.: Newton Methods for Nonlinear Problems. Springer Series in Computational Mathematics, vol 35. Springer, Berlin (2004)
13. Bellman, R.E.: The theory of dynamic programming. Bull. Am. Math. Soc. **60**, 503–515 (1954)
14. Falcone, M.: Numerical solution of dynamic programming equations. Appendix A in [21]
15. Falcone, M.: Numerical methods for differential games based on partial differential equations. Int. Game Theory Rev. **8**, 231–272 (2006)
16. Pontryagin, L.S., Boltyanski, V.G., Gamkrelidze, R.V., Mishtchenko, E.F.: The Mathematical Theory of Optimal Processes. Wiley–Interscience, New York (1962)
17. Bryson, A.E., Ho, Y.-C.: Applied Optimal Control. Hemisphere, New York (1975)
18. Pesch, H.J.: Real-time computation of feedback controls for constrained optimal control problems II: a correction method based on multiple shooting. Optim. Control Appl. Methods **10**, 147–171 (1989)
19. Bettiol, P., Frankowska, H.: Normality of the maximum principle for nonconvex constrained Bolza problems. J. Differ. Equ. **243**, 256–269 (2007)
20. Chitour, Y., Jean, F., Trélat, E.: Genericity results for singular curves. J. Differ. Geom. **73**, 45–73 (2006)
21. Bardi, M., Capuzzo Dolcetta, I.: Optimal Control and Viscosity Solutions of Hamilton-Jacobi-Bellman Equations. Birkhäuser, Boston (1997)
22. Cristiani, E., Falcone, M.: Fast semi-Lagrangian schemes for the Eikonal equation and applications. SIAM J. Numer. Anal. **45**, 1979–2011 (2007)
23. Bokanowski, O., Martin, S., Munos, R., Zidani, H.: An anti-diffusive scheme for viability problems. Appl. Numer. Math. **56**, 1147–1162 (2006)
24. Bokanowski, O., Cristiani, E., Zidani, H.: An efficient data structure and accurate scheme to solve front propagation problems. J. Sci. Comput. **42**, 251–273 (2010)
25. Tsai, Y.R., Cheng, L.T., Osher, S., Zhao, H.: Fast sweeping algorithms for a class of Hamilton-Jacobi equations. SIAM J. Numer. Anal. **41**, 673–694 (2003)

26. Bardi, M., Falcone, M., Soravia, P.: Fully discrete schemes for the value function of pursuit-evasion games. In Basar, T., Haurie, A. (eds) Advances in Dynamic Games and Applications, Annals of the International Society of Dynamic Games, vol. 1, pp. 89–105 (1994)
27. Soravia, P.: Estimates of convergence of fully discrete schemes for the Isaacs equation of pursuit-evasion differential games via maximum principle. SIAM J. Control Optim. **36**, 1–11 (1998)
28. More, J.J., Garbow, B.S., Hillstrom, K.E.: User Guide for MINIPACK-1. Argonne National Laboratory Report ANL-80-74 (1980)
29. Hairer, E., Nørsett, S.P., Wanner, G.: Solving Ordinary Differential Equations I. Springer Series in Computational Mathematics, vol. 8. Springer, Berlin (1993)
30. Gergaud, J., Martinon, P.: Using switching detection and variational equations for the shooting method. Optim. Control Appl. Methods **28**, 95–116 (2007)
31. Goddard, R.H.: A method of reaching extreme altitudes. Smithsonian Inst. Misc. Coll. **71** (1919)
32. Maurer, H.: Numerical solution of singular control problems using multiple shooting techniques. J. Optim. Theory Appl. **18**, 235–257 (1976)
33. Oberle, H.J.: Numerical computation of singular control functions in trajectory optimization. J. Guid. Control Dyn. **13**, 153–159 (1990)
34. Tsiotras, P., Kelley, H.J.: Drag-law effects in the Goddard problem. Automatica **27**, 481–490 (1991)
35. Seywald, H., Cliff, E.M.: Goddard problem in presence of a dynamic pressure limit. J. Guid. Control Dyn. **16**, 776–781 (1993)
36. Bonnans, F., Martinon, P., Trélat, E.: Singular arcs in the generalized Goddard's problem. J. Optim. Theory Appl. **139**, 439–461 (2008)
37. Camilli, F., Falcone, M., Lanucara, P., Seghini, A.: A domain decomposition method for Bellman equations. In: Keyes, D.E., Xu, J. (eds.) Domain Decomposition Methods in Scientific and Engineering Computing. Contemporary Mathematics, vol. 180, pp. 477–483. AMS, Providence (1994)